

Stability, structure and dynamics of cationic lanthanide(III) complexes of *N,N'*-bis(propylamide)ethylenediamine-*N,N'*-diacetic acid

Carlos Platas-Iglesias,^{a,b} Daniele M. Corsi,^a Luce Vander Elst,^c Robert N. Muller,^c Daniel Imbert,^d Jean-Claude G. Bünzli,^d Éva Tóth,^e Thomas Maschmeyer^a and Joop A. Peters^{*a}

^a Laboratory of Applied Organic Chemistry and Catalysis, Delft University of Technology, Julianalaan 136, 2628 BL Delft, The Netherlands. E-mail: j.a.peters@tnw.tudelft.nl; Fax: (+31) 15 2784289

^b Departamento de Química Fundamental, Universidade da Coruña, Campus da Zapateira s/n, 15071 A Coruña, Spain

^c NMR Laboratory, Department of Organic Chemistry, University of Mons-Hainaut, 7000 Mons, Belgium

^d Laboratory of Supramolecular Lanthanide Chemistry, Institute of Molecular and Biological Chemistry, Swiss Federal Institute of Technology Lausanne, BCH, CH-1015 Lausanne, Switzerland

^e Laboratory of Inorganic and Bioinorganic Chemistry, Institute of Molecular and Biological Chemistry, Swiss Federal Institute of Technology Lausanne, BCH, CH-1015 Lausanne, Switzerland

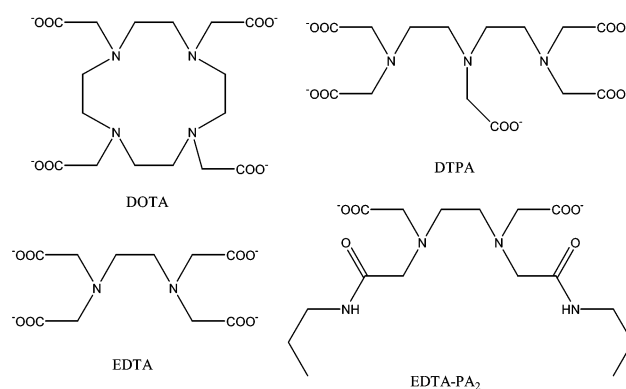
Received 11th November 2002, Accepted 18th December 2002

First published as an Advance Article on the web 28th January 2003

The cationic [Ln(EDTA-PA₂)]⁺ complexes (EDTA-PA₂ = EDTA-bispropylamide) have been characterised by a multinuclear NMR study. ⁸⁹Y and ¹³C NMR data indicate the formation of 1 : 1 and 1 : 2 (Ln : ligand) complexes in aqueous solution. The stability constants of these complexes, as determined by potentiometric measurements, are log *K*_{GdL} = 10.3 and log *K*_{GdL} = 14.3. ¹³C Relaxation times of the Nd³⁺ complex show hexadentate binding of the organic ligand *via* the two amines, the two carboxylates and the two amide oxygen atoms. The complexes are present in solution as a mixture of three isomers: two *trans* forms and a *cis* one. Luminescence measurements demonstrate that both Eu³⁺ and Tb³⁺ complexes are nona-coordinated at low concentrations (~10⁻³ M). Three water molecules then complete the coordination sphere. At higher concentrations, the complexes exist in solution as a mixture of nona- and octa-coordinated species, the relative concentration of the latter increases with increasing concentration as a consequence of intermolecular interactions operating in aqueous solutions. Data sets obtained from variable-temperature ¹⁷O NMR at 7.05 T and variable-temperature ¹H nuclear magnetic relaxation dispersion (NMRD) on the Gd³⁺ complex were fitted simultaneously to give insight into the parameters governing the water ¹H relaxivity. Fast rotation limits the relaxivity at 10–40 MHz.

Introduction

Gadolinium complexes with poly(aminocarboxylate) ligands present considerable interest since they are commonly used as contrast agents in magnetic resonance imaging (MRI).^{1–3} Currently, about a third of all MRI scans are made after administration of a Gd³⁺-based contrast agent. Contrast agents enhance the image contrast by preferentially influencing the relaxation efficiency of the water proton nuclei in the target tissue. The efficiency of a contrast agent is evaluated in terms of the relaxivity, which is defined as the relaxation-rate enhancement of water proton nuclei per mM concentration of the metal ion. These complexes contain at least one Gd³⁺-bound water molecule that rapidly exchanges with the bulk water of the body; this imparts an efficient mechanism for the longitudinal and transverse-relaxation (*T*₁ and *T*₂) enhancement of water protons. Around a paramagnetic ion, the relaxation rate of the bulk water protons is enhanced due to long-range interactions (outer-sphere relaxation) and short-range interactions (inner-sphere relaxation). According to the standard Solomon–Bloembergen–Morgan model, the latter process is governed by four correlation times: the rotational correlation time of the complex (τ_R), the residence time of a water proton in the inner coordination sphere (τ_m), and the electronic longitudinal and transverse relaxation rates ($1/T_{1e}$ and $1/T_{2e}$) of the metal centre.



Scheme 1

The two most studied ligand frameworks for Gd³⁺ complexes with poly(aminocarboxylates) are based on DOTA and DTPA^{1–3} (see Scheme 1). An important point that has to be understood when one wants to design new potential Gd-based contrast agents is the relationship between the structure and the parameters governing the relaxivity. Therefore, the study of the solution structure as well as the parameters governing the proton relaxivity of any Gd³⁺ polycarboxylate complex is interesting for the rational design of novel and more efficient

contrast agents for MRI. For instance, the ideal value of the residence time of water molecules in the inner coordination sphere, τ_m , can be calculated to be about 30 ns at 25 °C, but both Gd(DOTA)⁻ and Gd(DTPA)²⁻, the two reference compounds that first became available for clinical use, have τ_m values of about 300 ns.⁴ This value further increases by an order of magnitude for derivatives in which carboxylate groups of the ligands are replaced by carboxamide moieties.⁴ In the search for a better understanding of the relationship between the exchange rate of the coordinated water and the structure and overall electric charge of the complex we report here a detailed study of the structure and dynamics in aqueous solution of cationic Ln³⁺ complexes with the polycarboxylate ligand EDTA-PA₂ (Scheme 1). Although lanthanide complexes of EDTA⁴⁻ have been studied extensively in the past,⁵⁻⁷ less is known about the coordination chemistry of functionalised EDTA derivatives.^{8,9} In the present study the structures and dynamics of the EDTA-PA₂ complexes was investigated by potentiometry, multinuclear (⁸⁹Y, ¹³C, ¹⁷O, ²H) NMR, UV-visible and luminescence spectroscopy to give detailed information on the structure, the dynamics, and the stability of the species in solution. Nuclear magnetic resonance dispersion (NMRD) investigations and variable-temperature ¹⁷O NMR measurements of the Gd(EDTA-PA₂)⁺ complex were conducted in order to assess its relaxation enhancement abilities and to gain insight into the parameters which govern the relaxation process in this positively charged complex.

Results and discussion

Chemical speciation in aqueous solution, protonation constants and thermodynamic stability constants

The chemical properties and the ionic radius of Y³⁺ for a coordination number of 9 (1.08 Å) are comparable to those of the Ln³⁺ ions (1.22–1.03 Å), and thus Y³⁺ complexes have coordination numbers and geometries that are closely related to those of the Ln³⁺ complexes. The formation of the Y³⁺ complexes with EDTA-PA₂ was monitored by ⁸⁹Y NMR in a 0.15 M YCl₃ solution in D₂O at pD 6.0. The spectrum recorded on a solution with $\rho' = 0.5$ (where ρ' is the molar ratio EDTA-PA₂ : Y³⁺) displays a signal at about 0 ppm due to free Y³⁺ as well as two sharp signals at 100.6 and 102.3 ppm that can be assigned to the presence of two [Y(EDTA-PA₂)]⁺ isomers in aqueous solution. Upon increase of the amount of ligand at $\rho' = 1$, these two peaks coalesce to a single broad peak at 101.4 ppm, while the peak due to uncomplexed Y³⁺ is no longer observable. When more ligand is added to the solution the peak at 101.4 progressively shifts to higher fields until 90.5 ppm for $\rho' = 2$ reflecting the formation of 1 : 2 (Y³⁺ : L) species in solution, as observed before for related systems.^{8,9} ¹³C NMR data confirmed the formation of both 1 : 1 and 1 : 2 species in aqueous solution: when increasing amounts of NdCl₃·6H₂O were added to a D₂O solution of EDTA-PA₂ at 25 °C (pD = 6.0), the ¹³C resonances of the ligand became broader, reflecting exchange processes between different species in solution, while for ρ' in the range 0.5–1.0, the ¹³C resonances gradually became sharper. Once the 1 : 1 stoichiometry was reached, addition of more NdCl₃·6H₂O did not result in further changes in the spectrum.

The ligand protonation constants K_i and the stability constants of the Gd³⁺ complexes β_{ML} were determined by pH-potentiometry:

$$K_i = \frac{[H_iL]}{[H_{i-1}L][H^+]} \quad (1)$$

$$\beta_{ML_i} = \frac{[ML_i]}{[M][L]^i} \quad (2)$$

Table 1 Ligand protonation constants and thermodynamic stability constants of EDTA-PA₂ and its Gd³⁺ complexes as determined by pH-potentiometry ($I = 0.1$ M (CH₃)₄NCl). Data reported previously for related systems are provided for comparison

	EDTA-PA ₂	EDTA-IPA ₂ ^{a,c}	EDTA-TBA ₂ ^{b,c}	EDTA ^d
pK ₁	7.15 ± 0.01	7.36	7.19	10.17
pK ₂	3.59 ± 0.01	3.66	3.81	6.11
pK ₃	1.96 ± 0.03	1.99	1.95	2.68
pK ₄				1.95
β_{ML}	10.3 ± 0.1	12.79	12.76	17.32
β_{ML_2}	14.3 ± 0.2	18.96	20.35	

^a EDTA-bis(isopropyl)amide. ^b EDTA-bis-*tert*-butylamide. ^c From ref. 9. ^d From ref. 10.

These data are collected in Table 1 and compared with those of similar ligands.^{9,10} They clearly show that the stability of the [GdL]⁺ complexes (where L = EDTA-bisamide) is lower than that of [Gd(EDTA)]⁻.

Coordination of the EDTA-PA₂ ligand

The ¹³C NMR spectra of the diamagnetic La³⁺ and Lu³⁺ EDTA-PA₂ (1 : 1) complexes in D₂O at 25 °C display two sets of signals for the ¹³C nuclei of the EDTA backbone. The spectra of the paramagnetic complexes (Ce, Pr and Nd) show also a doubling of the number of resonances for the ¹³C nuclei in the propyl side chains (Table 2). These data point to the presence of at least two different isomers in aqueous solution.

Information on the coordination of the isomers by the Ln³⁺ ions was obtained from Nd³⁺ induced relaxation rate enhancements in the ¹³C nuclei of the EDTA-PA₂ ligand. Among the lighter Ln³⁺ ions (Ln = Ce→Eu), Nd³⁺ has the longest electron relaxation times,^{11,12} and therefore this cation is very suitable for obtaining structural information of lanthanide complexes in solution.¹³⁻¹⁵ The Nd³⁺-induced ¹³C NMR relaxation enhancements for EDTA-PA₂ were measured at 7.05 T and 25 °C (Table 3). In order to correct for diamagnetic contributions, the relaxation rates for the corresponding La³⁺ complex were subtracted from the measured values of the Nd³⁺ complex (see Table 3).

Under the conditions employed, the signals for each of the two isomers existing in solution were well resolved for some of the carbons, while for the carbons in the α -position with respect to the carbonyl groups and for the carbons of the ethylene bridge only one signal is observed. Therefore, the relaxation rates obtained in the latter case are averaged relaxations for the structures of the two isomers. Since the outer-sphere contribution ($1/T_{1,os}$) becomes significant only for remote nuclei this contribution was neglected. From the electron relaxation for Nd³⁺ ($T_{1e} \approx 10^{-13}$ s) it can be estimated that the contact contribution to the paramagnetic relaxation is negligible for this Ln³⁺ ion. Two contributions are of importance: the “classical” dipolar relaxation and the Curie relaxation. Eqn. (3) can be

$$\frac{1}{T_1} = \left[\frac{4}{3} \left(\frac{\mu_0}{4\pi} \right)^2 \mu^2 \gamma_I^2 \beta^2 T_{1e} + \frac{6}{5} \left(\frac{\mu_0}{4\pi} \right)^2 \frac{\gamma_I^2 H_0^2 \mu^4 \beta^4}{(3kT)^2} \tau_R \right] \frac{1}{r^6} \quad (3)$$

derived from a simplified Solomon–Bloembergen equation¹⁶ and the equation for the Curie relaxation.^{17,18} In this equation, the first term between the brackets represents the “classical” dipolar contribution, and the second term describes the Curie relaxation. Here, $\mu_0/4\pi$ is the magnetic permeability in a vacuum, μ is the effective magnetic moment of the lanthanide ion, γ_I is the gyromagnetic ratio of the nucleus under study, β is the Bohr magneton, T_{1e} is the electron spin relaxation time, r is the distance between the ¹³C nucleus in question and the lanthanide ion, H_0 is the magnetic field strength, k is the Boltzmann constant, T is the temperature, and τ_R is the

Table 2 ^{13}C NMR shifts for the $[\text{Ln}(\text{EDTA-PA}_2)]^+$ complexes in 0.165 M D_2O solutions at 25 °C and pD = 6.5

	COO	CONH	CH_2COO	CH_2CONH	$\text{NCH}_2\text{CH}_2\text{N}$	$\text{CH}_2\text{CH}_2\text{CH}_3$	$\text{CH}_2\text{CH}_2\text{CH}_3$	$\text{CH}_2\text{CH}_2\text{CH}_3$
La	181.2	175.5	63.2	61.5	55.9	43.1	23.2	12.2
	180.0	175.4		61.0	55.6		23.0	
Lu	181.1	176.9	64.0	62.2	59.4	43.6	22.9	12.2
	181.0		63.6	62.0				
Ce	185.4	171.6	59.2	52.8	37.1	45.7	24.4	13.3
	179.8	167.2	59.4		36.1	44.5	23.6	12.8
Pr	196.6	168.7	59.1	57.3	15.7	47.6	25.2	13.7
	181.1	154.2	45.7	41.0	16.0	43.9	23.2	12.7
Nd	180.9	167.7	54.6	45.5	22.1	46.5	24.3	13.2
	174.1	161.0				44.8	23.3	12.7

Table 3 ^{13}C NMR relaxation data (s^{-1}) for 165 mM solutions of Ln^{3+} complexes in D_2O at 25 °C and pD = 6

	$1/T_{1(\text{Nd})}$	$1/T_{1(\text{La})}$	$1/T_{1(\text{La-Nd})}^a$	$r/\text{\AA}$
COO	6.636	0.355	1.852	3.20
	7.189	0.294		
CONH	5.379	0.341	1.085	3.35
	5.388		1.217	
CH_2COO	10.526	3.340	3.805	3.16
		3.486		
CH_2CONH	7.262	3.448	3.593	3.53
		3.759	2.945	
$\text{NCH}_2\text{CH}_2\text{N}$	8.977	3.990	4.205	3.36
		4.078	4.440	
$\text{CH}_2\text{CH}_2\text{CH}_3$	2.160	1.766	1.800	5.10

^a Relaxation data (s^{-1}) for the ^{13}C NMR resonances of $[\text{La}(\text{EDTA-PA}_2)]^+$ in the presence of one equivalent of $[\text{Nd}(\text{EDTA-PA}_2)]^+$. The total concentration of Ln^{3+} ions was 170 mM.

rotational tumbling time of the complex. The contribution of the Curie spin mechanism to the total relaxation becomes significant for larger molecules (τ_R increases), particularly at higher fields. If τ_R and $T_{1,e}$ are known, the absolute distances between Nd^{3+} and the ligand nuclei can be calculated from the relaxation rates by using eqn. (3).

The relative Nd^{3+} -C distances for $[\text{Nd}(\text{EDTA-PA}_2)]^+$ were calculated from the paramagnetic relaxation rates (see Table 3) by using eqn. (3). A τ_R value of 171 ps, as determined from the deuterium longitudinal relaxation rate of the diamagnetic $[\text{La}(\text{EDTA-PA}_2)]^+$ complex with the deuterated ligand (see below), was used in these calculations. From these data it is clear that the organic ligand is bound in a similar fashion as EDTA, *i.e.* through the two carboxylate groups acting as monodentate anions, the two amide oxygen atoms, and the two nitrogen atoms. The distances presented in Table 3 are normalised with respect to a distance between the carbon atoms of the carboxylate groups and Nd^{3+} , which was assumed to be 3.2 Å. By fixing this distance, a $T_{1,e}$ value of 4.22×10^{-14} s was calculated from eqn. (3). This is close to the $T_{1,e}$ data reported by Alsaadi *et al.*¹¹ on Nd^{3+} complexes, particularly if one considers that, as a result of the r^6 dependence shown in eqn. (3), an error of 5% in the distances leads to an error of 34% in $T_{1,e}$. The propyl carbon atoms at position β and γ with respect to the amide function are relatively far away from the Nd^{3+} ion. Consequently, their Nd^{3+} -induced relaxation rate enhancement is small causing the corresponding Nd^{3+} -C distances to be inaccurate; hence, these data were not considered. All calculated distances are in the range previously observed for Nd^{3+} complexes of DTPA-bis-amides.^{14,15}

Isomer interconversion in $[\text{Ln}(\text{EDTA-PA}_2)]^+$

Upon hexadentate binding of EDTA-PA₂ to Ln^{3+} ions inversion of the two nitrogen atoms of the ligand backbone is precluded. Consequently, the two nitrogen atoms become chiral. Furthermore, the coordinated ethylenediamine unit may adopt

two different stable conformations, δ and λ .¹⁹ Therefore, in principle, eight enantiomeric forms are possible in the static situation. Between 0 and 85 °C, only two sets of resonances were observed in the ^{13}C spectra. Most likely, the wagging motion between the δ and λ form is rapid on the NMR time scale under these conditions. Moreover, it is likely that the *R,S/S,R*-isomers have a geometry with nearly C_2 symmetry and, therefore, cannot be discriminated by NMR. So, three “time-averaged” complex geometries remain to be considered (see Fig. 1): two *trans* (*R,R* and *S,S*) and one *cis* (*R,S*). The two *trans* isomers are mirror images and are thus not distinguishable by NMR.

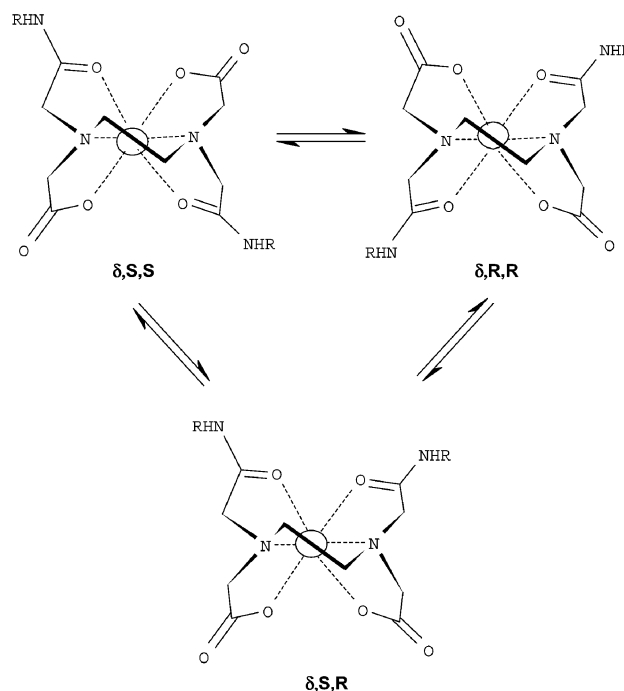


Fig. 1 Schematic representation of the isomers of the $\text{Ln}(\text{EDTA-PA}_2)^+$ complexes: $\text{R} = \text{CH}_2\text{CH}_2\text{CH}_3$. Only the enantiomers with a δ -configuration of the ethylenediamine unit are depicted.

Upon increasing the temperature of a sample of the diamagnetic $[\text{La}(\text{EDTA-PA}_2)]^+$ complex from 25 to 85 °C, a substantial increase of the line widths was observed in the ^{13}C spectrum, and the two sets of signals coalesced at 85 °C. If it is assumed that the exchange process associated with this line broadening (before coalescence) is slow on the NMR time scale, then the exchange rate between the *cis* and *trans* isomers (k) can be calculated from the observed line widths ($\Delta\nu_{1/2}$):

$$k = \pi(\Delta\nu_{1/2} - \Delta\nu_{1/2}(0)) \quad (4)$$

where $\Delta\nu_{1/2}(0)$ is the linewidth in the absence of exchange. A plot of k/T versus $1/T$ [$k = (k_b T/h) \exp((\Delta S^\ddagger/R) - (\Delta H^\ddagger/RT))$] (where k_b and h are the Boltzmann and Planck constants,

respectively, T is the absolute temperature and k is the rate constant) yields the activation parameters for the interconversion process ($\Delta G^\ddagger = 78 \pm 5 \text{ kJ mol}^{-1}$, $\Delta H^\ddagger = 84 \pm 5 \text{ kJ mol}^{-1}$, $\Delta S^\ddagger = 19 \pm 16 \text{ J mol}^{-1} \text{ K}^{-1}$, $k = 0.12 \pm 0.02 \text{ s}^{-1}$ at 298 K). The calculated ΔG^\ddagger is comparable to those determined for the inversion of the terminal diethylenetriamine N-atoms in lanthanide complexes with DTPA bis-amide derivatives, which requires partial decoordination of the ligand.^{14,15} This confirms that the two isomers of $[\text{Ln}(\text{EDTA-PA}_2)]^+$ evidenced in the ^{13}C NMR spectra are the *cis* and *trans* forms that interconvert by inversion of the terminal ethylenediamine N-atoms.

Self-association

The value of the rotational correlation time, τ_R , can be estimated from the analysis of the deuterium longitudinal relaxation rate of the deuterated ligand complexed to the diamagnetic La^{3+} ion.²⁰ In diamagnetic systems the deuterium relaxation is fully controlled by quadrupolar interactions. Under the extreme narrowing condition ($\omega\tau_R \ll 1$), it is given by eqn. (5).

$$R_1 = \frac{1}{T_1} = \frac{3}{8} \left(\frac{e^2 q Q}{\hbar} \right)^2 \tau_R \quad (5)$$

The quadrupolar coupling constant ($e^2 q Q / \hbar$) depends on the degree of hybridisation of the C–H bond, and takes a value of approximately $170 \cdot 2\pi \text{ kHz}$ for a $\text{C}_{(\text{sp}^3)}\text{–H}$ bond.^{21,22} The T_1 values for aqueous solutions of the $[\text{La}(\text{EDTA-PA}_2\text{-}d_4)]^+$ complex appeared to increase upon dilution of the solution, while the calculated τ_R values decrease linearly (Fig. 2). This effect was

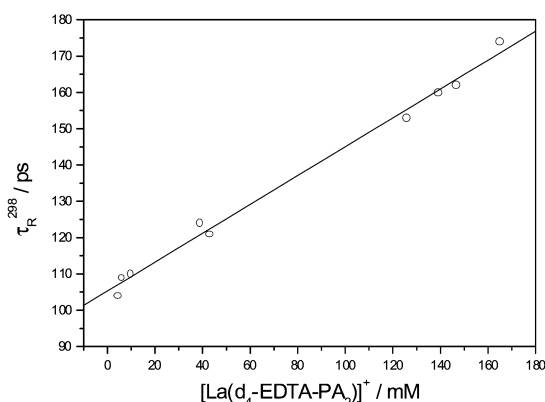


Fig. 2 Rotational correlation times at 298 K (τ_R^{298}) obtained with H_2O solutions of $[\text{La}(\text{EDTA-PA}_2\text{-}d_4)]^+$ at different concentrations.

previously observed for different polycarboxylate chelates,²⁰ and it has been attributed to an increase of intermolecular interactions and viscosity in concentrated solutions. A rotational correlation time of 104 ps was determined for the $[\text{La}(\text{EDTA-PA}_2\text{-}d_4)]^+$ complex at a concentration close to those generally used for NMRD studies (4 mM). This rotational correlation time is longer than those reported in the literature for small Ln^{3+} complexes (66 ps for $[\text{Ln}(\text{DTPA-BMA})]$, BMA = bismethylamine; 58 ps for $[\text{Ln}(\text{DTPA})]^{2-}$ and 66 ps for $[\text{La}(\text{EDTA})]^{-4,23}$ and, therefore, we suspected that self-association occurs in this system. To further explore the possibility of intermolecular interactions in the $[\text{Ln}(\text{EDTA-PA}_2)]^+$ complexes, we have performed a titration of a solution of the diamagnetic $[\text{La}(\text{EDTA-PA}_2)]^+$ with the paramagnetic $[\text{Tm}(\text{EDTA-PA}_2)]^+$. Upon addition of increasing amounts of Tm^{3+} complex to the $[\text{La}(\text{EDTA-PA}_2)]^+$ solution most of the ^{13}C resonances of the La^{3+} complex shift linearly to lower fields (Fig. 3). The exchange between the La^{3+} and the Tm^{3+} complex was slow on

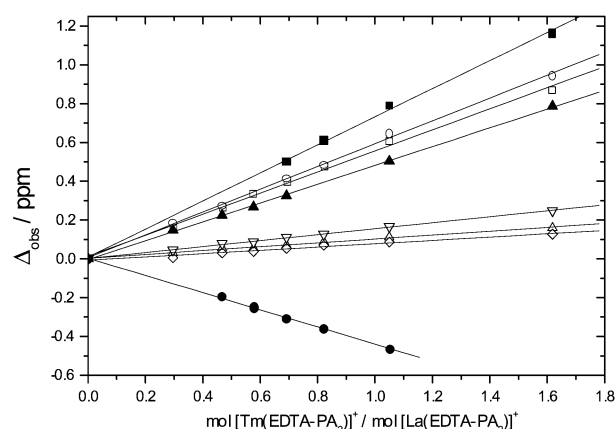


Fig. 3 ^{13}C NMR shifts induced in $[\text{La}(\text{EDTA-PA}_2)]^+$ upon addition of $[\text{Tm}(\text{EDTA-PA}_2)]^+$: CH_2COO^- (■, ●); $-\text{CH}_2\text{CH}_2-$ (○); $-\text{CH}_2\text{CONH}-$ (□); $-\text{CH}_2\text{CONH}-$ (▲); $\text{CH}_2\text{CH}_2\text{CH}_3$ (▽); $\text{CH}_2\text{CH}_2\text{CH}_3$ (Δ); $\text{CH}_2\text{CH}_2\text{CH}_3$ (◇). The concentration of $[\text{La}(\text{EDTA-PA}_2)]^+$ was 179 mM at pD = 6.

the NMR timescale. Assuming that no covalent interactions are involved and that the diamagnetic shifts are insignificant, only pseudo-contact contributions have to be considered.

The relative large induced shifts indicate that the nuclei of the molecule must approach the paramagnetic Ln^{3+} ion rather closely and must have a preferential orientation. Without a preferred orientation, the nuclei would experience all possible orientations equally and the pseudo-contact shift would average to zero. A preferred location is supported by the different signs and magnitudes of the induced shifts for the various nuclei in the $[\text{La}(\text{EDTA-PA}_2)]^+$ complex, which shows that the various nuclei have different location with respect to the lanthanide ion and the magnetic axes.²

The ^{13}C resonance of the carboxylic functions immediately disappeared upon addition of small amounts of Tm^{3+} complex to the La^{3+} one, probably because it is too broad to be detected. This indicates that the $[\text{La}(\text{EDTA-PA}_2)]^+$ complex is interacting with $[\text{Tm}(\text{EDTA-PA}_2)]^+$ through the carboxylic groups. This is confirmed by the longitudinal ^{13}C relaxation enhancement effects induced in $[\text{La}(\text{EDTA-PA}_2)]^+$ by addition of an equimolar amount of $[\text{Nd}(\text{EDTA-PA}_2)]^+$ (Table 3). The relaxation rate of the ^{13}C resonance of the carbonyl group was enhanced by a factor of 5.2, that of the carbonyl group of the amide functions was enhanced by a factor of 3.2, whereas the relaxation rates for other carbon resonances of the ligand were nearly not affected. This suggests that the carboxyl groups are involved in the formation of the intermolecular adducts, most likely *via* intermolecular bridging of the monomeric complexes.

Hydration numbers

Emission and absorption spectra. The emission spectrum of a 10^{-3} M solution of $[\text{Eu}(\text{EDTA-PA}_2)]^+$ in D_2O at pD 6 and 295 K, obtained under excitation at $25\,253 \text{ cm}^{-1}$, displays the typical $^5\text{D}_0 \rightarrow ^7\text{F}_j$ transitions. The spectrum is dominated by the transition to $^7\text{F}_2$, as shown by the integrated and corrected relative intensities: 0.41, 1.00, 1.76 and 0.47 for $J = 0, 1, 2$ and 4. The $^5\text{D}_0 \leftarrow ^7\text{F}_0$ excitation spectrum of the same solution recorded by monitoring in the maximum of the transition to $^7\text{F}_2$ produces a single band with a maximum at $17\,253 \text{ cm}^{-1}$. This band is fairly sharp (full width at half-height $\text{fwhm} = 8.7 \text{ cm}^{-1}$) and presents a faint shoulder on the low energy side. Moreover, the excitation spectra recorded by analysing at different emission wavelengths are virtually identical to that one, which is consistent with the presence of a single main environment for Eu^{3+} in the complex.

The emission lifetimes of the $\text{Eu}(^5\text{D}_0)$ and $\text{Tb}(^5\text{D}_4)$ excited levels have been measured in D_2O and H_2O (10^{-3} M solutions)

and were used to calculate the number of coordinated water molecules q by use of eqns. (6) and (7):

$$q = 1.05(\Delta k_{\text{obs}}) \quad (6a)$$

$$q = 1.2(\Delta k_{\text{obs}} - 0.25 - 0.075q^N) \quad (6b)$$

$$q = 1.11(\Delta k_{\text{obs}} - 0.31 - 0.075q^N) \quad (6c)$$

$$q = 4.2(\Delta k_{\text{obs}}) \quad (7a)$$

$$q = 5.0(\Delta k_{\text{obs}} - 0.06) \quad (7b)$$

where $k_{\text{obs}} = 1/\tau_{\text{obs}}$, $\Delta k_{\text{obs}} = k_{\text{obs}}(\text{H}_2\text{O}) - k_{\text{obs}}(\text{D}_2\text{O})$, k_{obs} is given in ms^{-1} and q^N is the number of NH oscillators when amide groups are coordinated to the metal ion. The measured emission lifetimes in H_2O solutions ($\tau_{\text{obs}}(\text{H}_2\text{O})$) are 0.28 ± 0.01 (Eu) and 0.98 ± 0.01 ms (Tb), while the $\tau_{\text{obs}}(\text{D}_2\text{O})$ values amount to 2.33 ± 0.01 (Eu) and 3.04 ± 0.01 ms (Tb). By using eqns. (6a) and (7a),²⁴ we obtain $q = 3.3$ and 2.9 for Eu and Tb, respectively, with an estimated uncertainty on q of ± 0.5 . These equations were established from crystalline complexes in which interactions generated by molecules of water in the second coordination sphere are absent. Consequently, we have also made use of eqns. (6b) and (7b), proposed by Beeby *et al.*²⁵ for solutions of polyaminocarboxylate complexes with $q \leq 1$ (including cyclen derivatives), with $q^N = 2$ and obtained $q = 3.3$ and 3.2 for Eu and Tb, respectively. Therefore, eqns. (6a,b) and (7a,b) give similar results with an average number $q = 3.3$ (Eu) and 3.0 (Tb). Quite recently, a refined equation (6c),²⁶ has been proposed for Eu complexes in solution, with an estimated uncertainty on q of ± 0.1 . In our case, this equation yields $q = 3.0$ for the Eu complex. All these results point to the complexes having three coordinated water molecules in aqueous solutions at this concentration.

The absorption spectrum of a 6.25×10^{-3} M solution of $[\text{Eu}(\text{EDTA-PA}_2)]^+$ recorded in the ${}^5\text{D}_0 \leftarrow {}^7\text{F}_0$ region presents a main band centred at about 17260 cm^{-1} as well as a faint shoulder on the low energy side (Fig. 4(a)), in agreement with the excitation spectrum. On the basis of the emission lifetimes of the Eu and Tb complexes, the absorption band appearing at high energy can be safely assigned to the species with $q = 3$. The presence of two absorption bands in this region has been previously observed for other Eu^{3+} chelates such as $[\text{Eu}(\text{EDTA})]^-$,⁷ and has been attributed to an equilibrium between species with two and three inner-sphere water molecules. Several evidences suggest that this is also the case for the $[\text{Eu}(\text{EDTA-PA}_2)]^+$ chelate: (i) The absorption spectra of $[\text{Eu}(\text{EDTA-PA}_2)]^+$ are nearly identical to those reported for $[\text{Eu}(\text{EDTA})]^-$;⁷ (ii) The variation with temperature of the UV-visible absorption spectra of $[\text{Eu}(\text{EDTA-PA}_2)]^+$ can be explained very well with an equilibrium between a nine-coordinate species containing three inner-sphere water molecules and an eight-coordinate species with two inner-sphere water molecules: the intensity of the band at 17260 cm^{-1} decreases with increasing temperature while that of the band at 17246 cm^{-1} increases; (iii) The low energy band is assigned to $[\text{Eu}(\text{EDTA-PA}_2)(\text{H}_2\text{O})_2]^+$ in line with the smaller nephelauxetic effect for this species compared to $[\text{Eu}(\text{EDTA-PA}_2)(\text{H}_2\text{O})_3]^+$.²⁷ Therefore, an equilibrium between $[\text{Eu}(\text{EDTA-PA}_2)(\text{H}_2\text{O})_3]^+$ and $[\text{Eu}(\text{EDTA-PA}_2)(\text{H}_2\text{O})_2]^+$ species appears to exist also in the case of the EDTA-PA₂ (L) derivatives:



Upon increasing the concentration the relative intensity of the absorption bands changes dramatically (Fig. 4), the absorption assigned to the $[\text{Eu}(\text{EDTA-PA}_2)(\text{H}_2\text{O})_2]^+$ species grows at the expense of that attributed to $[\text{Eu}(\text{EDTA-PA}_2)(\text{H}_2\text{O})_3]^+$. This is, to the best of our knowledge, the first time that such a con-

Table 4 Thermodynamic parameters determined by UV-visible spectrophotometry for equilibrium (9) at pH = 6

$[\text{Eu}^{3+}]/\text{M}$	Ligand	K^{298}	ΔH° ^a	ΔS° ^b
0.1	EDTA-PA ₂	0.44 ± 0.04		
0.05		0.35 ± 0.04		
0.025		0.23 ± 0.03		
0.0125		0.15 ± 0.04		
0.009		0.031 ± 0.009	22 ± 4	46 ± 11
0.00625	EDTA	0.085 ± 0.008		
0.0201		0.59 ± 0.05	17.7 ± 0.5	54.9 ± 1.6

^a Data in kJ mol^{-1} . ^b Data in $\text{J K}^{-1} \text{mol}^{-1}$.

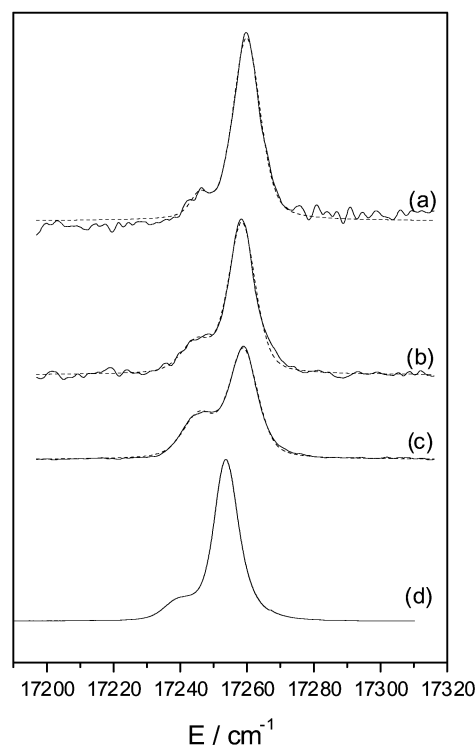


Fig. 4 UV-visible spectra of the $\text{Eu}^{3+} {}^5\text{D}_0 \leftarrow {}^7\text{F}_0$ transition in $[\text{EuEDTA-PA}_2]^+$ recorded at different concentrations at 298 K and pH = 5.8: (a) 6.25×10^{-3} M; (b) 0.025 M and (c) 0.1 M. The dotted lines correspond to the best least-squares fit of the experimental data as described in the text. Spectrum (d): Excitation spectrum of the ${}^5\text{D}_0 \rightarrow {}^7\text{F}_0$ transition in $[\text{EuEDTA-PA}_2]^+$ (analysis wavelength: 16257 cm^{-1} ; concentration: 0.1 M). Vertical scale: arbitrary units.

centration dependence of the number of inner-sphere water molecules has been observed. This phenomenon has to be traced back to the presence of intermolecular interactions in aqueous solutions at higher concentrations (*vide supra*). A previously reported least squares fitting procedure⁷ was used to determine the equilibrium constants according to eqn. (8) at different concentrations. Furthermore, the temperature dependence of the absorption spectrum at a concentration of 0.009 M was used to determine the reaction enthalpy, ΔH° , and reaction entropy, ΔS° . The results are compiled in Table 4. For comparison, previously reported data for EDTA⁷ are included in this Table. It should be noted that the intermolecular interactions observed between the monomeric chelates may also lead to a decrease in the hydration number. Therefore, one could argue that the second absorption band in the UV-Vis spectrum is to be attributed to the aggregated species. However, the variable temperature UV-Vis study performed at 0.009 M concentration and 1 : 1 metal/ligand ratio seems to disprove this. The lower intensity absorption band increases with increasing temperature, whereas the self-aggregation should be more important at lower temperatures resulting in an opposite temperature dependence.

Table 5 Lanthanide-induced water ^{17}O shifts (ppm) for 0.2 M $[\text{Ln}(\text{EDTA-PA}_2)]^+$ complexes in D_2O at pD 6

Ln^{3+}	$\delta^{a,b}/\text{ppm}$	$\delta^{a,c}/\text{ppm}$	Ln^{3+}	$\delta^{a,b}/\text{ppm}$	$\delta^{a,c}/\text{ppm}$
La	252	-221	Ho	-4777	-4370
Ce	473	0	Er	-2620	-2620
Pr	838	260	Tm	-1218	-1461
Nd	1157	430	Yb	-205	-656
Tb	-6336	-5229	Lu	241	-321
Dy	-5531	-4699			

^a The values are extrapolated to a molar ratio of $\text{Ln}^{3+}/\text{water}$ (ρ_w) = 1.
^b Values obtained at 25 °C. ^c Values obtained at 73 °C.

Ln^{3+} -Induced water ^{17}O shifts. Previously, we have shown that the Dy^{3+} -induced water ^{17}O shift is almost independent of the other ligands coordinated to the Dy^{3+} ion.^{28–31} Consequently the Dy^{3+} -induced shift can be used to determine the hydration numbers of the Dy^{3+} complexes. The Dy^{3+} -induced shift as measured for the $[\text{Dy}(\text{EDTA-PA}_2)]^+$ system at 25 °C (extrapolated to a molar ratio of $\text{Dy}^{3+}/\text{water}$ (ρ_w) = 1) amounts 5531 ppm. The Dy^{3+} -induced shift determined for a DyCl_3 solution under the same conditions amounts to 20358 ppm. If it is assumed that in the absence of organic ligands Dy^{3+} is coordinated to eight water ligands, it can be concluded from these data that $q = 2.2$. From the data reported in Table 4, we can estimate a $K^{298} \approx 0.5\text{--}0.6$ at the concentration used for investigating the Ln^{3+} -induced ^{17}O NMR shifts (0.2 M). Therefore, the averaged number of bound molecules is estimated to be in the range 2.6–2.7. This is in good agreement with the experimental (averaged) value of 2.2 since the eight coordinated species is expected to be more favoured upon the decrease of the ionic radius upon going from Eu^{3+} to Dy^{3+} .

In order to evaluate the number of inner-sphere water molecules in the other $[\text{Ln}(\text{EDTA-PA}_2)]^+$ complexes, a more rigorous treatment of the Ln^{3+} -induced water ^{17}O shifts is required. The induced shifts (Δ) are a combination of diamagnetic (Δ_d), contact (Δ_c) and pseudo-contact (Δ_p) shifts. The value of Δ_d was estimated from the induced shift of the La^{3+} complex for the lighter lanthanide complexes ($\text{Ce}\rightarrow\text{Eu}$) and from the induced shift of the Lu^{3+} complex for the heavier lanthanide complexes ($\text{Tb}\rightarrow\text{Yb}$). The contact contribution results from a through-bond transmission of unpaired density of the Ln^{3+} cation in question, whereas the pseudo-contact shift arises from a through-space dipolar interaction between the magnetic moments of the unpaired electrons of the Ln^{3+} electrons and any NMR active nucleus. Both Δ_c and Δ_p can be expressed as the product of a term characteristic of the Ln^{3+} ion but independent of the complex structure ($\langle S_z \rangle$ and C^D , respectively) and a second term characteristic of the complex but independent of the Ln^{3+} ion (F and G , respectively):^{32–34}

$$\Delta' = \Delta - \Delta_d = \Delta_c + \Delta_p = \langle S_z \rangle F + C^D G \quad (9)$$

Values for $\langle S_z \rangle$ and C^D are tabulated in the literature.³⁴ When the various Ln^{3+} complexes are isostructural, eqn. (9) can be rearranged in a linear form:^{32–34}

$$\Delta'/C^D = \frac{\langle S_z \rangle F}{C^D} + G \quad (10)$$

So, when a series of Ln^{3+} complexes yields a linear plot of Δ'/C^D versus $\langle S_z \rangle/C^D$, this is an indication that they are isostructural.² The water ^{17}O shifts obtained for the various $[\text{Ln}(\text{EDTA-PA}_2)]^+$ systems at 25 and 73 °C were extrapolated to $\rho_w = 1$ (see Table 5). The values obtained correspond to $q\Delta$ where q is the number of inner-sphere water molecules. Plots according to eqn. (10) give single straight lines for the whole series of

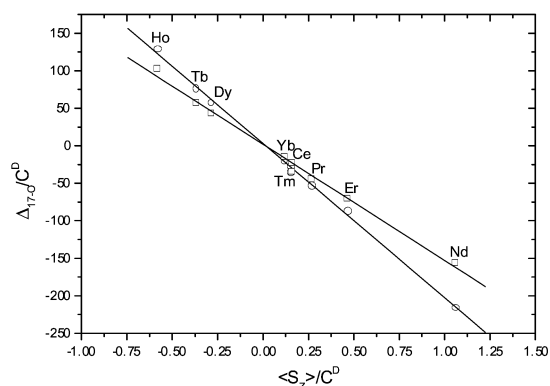


Fig. 5 Plot of Δ'/C^D versus $\langle S_z \rangle/C^D$ for the ^{17}O signal in the $[\text{Ln}(\text{EDTA-PA}_2)]^+$ system at 25 (○) and 73 °C (□).

lanthanide complexes at both temperatures (Fig. 5). By means of a multiple least-squares method the values of qF were determined to be $-206(3)$ and $-155(5)$ at 25 and 73 °C, respectively, while the values of qG were $3(2)$ and $2(2)$, respectively. The qF values are proportional to the inverse of the temperatures, as should be expected for contact shifts.³¹ It may be concluded that the q value remains fairly constant along the lanthanide series and does not change much with the temperature. However, we cannot exclude that a small and gradual change in the hydration number occurs along the lanthanide series, which cannot be detected in the plots according to eqn. (10).

The parameters determining the relaxivity

The relaxivity describes the efficiency of magnetic dipolar coupling occurring between the solvent nuclei and the paramagnetic metal ion and represents a measure of the efficacy of the complex as a contrast agent. The relaxation rates of the bulk water protons in the vicinity of a paramagnetic ion are enhanced due to long-range interactions (outer-sphere relaxation) and short-range interactions (inner-sphere relaxation). The latter are governed by the rotational correlation time of the complex (τ_R), the residence time of a water proton in the inner coordination sphere (τ_m), and the electronic longitudinal and transverse relaxation rates ($1/T_{1e}$ and $1/T_{2e}$) at the metal centre. As pointed out previously,⁴ it is difficult to determine the parameters determining the relaxivity of a given compound from nuclear magnetic resonance dispersion (NMRD) profiles without obtaining independent information of at least some of the most important parameters. We therefore carried out variable-temperature ^{17}O NMR measurements in solutions of the Gd^{3+} complex to obtain information about the water exchange kinetics. Furthermore, the rotational correlation times were determined independently from the ^2H transversal relaxation rates in the La^{3+} complexes of the deuterated ligand (see above).

Variable-temperature ^{17}O NMR measurements. A 37 mM aqueous solution of the $[\text{Gd}(\text{EDTA-PA}_2)]^+$ chelate was investigated by variable-temperature ^{17}O NMR shifts and relaxation measurements. From the measured ^{17}O NMR relaxation rates and angular frequencies of the $[\text{Gd}(\text{EDTA-PA}_2)]^+$ solution, $1/T_1$, $1/T_2$ and ω , and of the acidified water reference $1/T_{1A}$, $1/T_{2A}$ and ω_A , one can calculate the reduced relaxation rates and chemical shifts, $1/T_{1r}$, $1/T_{2r}$, and ω_r , which may be written as eqns. (11)–(13):^{35–38}

$$\frac{1}{T_{1r}} = \frac{1}{P_m} \left[\frac{1}{T_1} - \frac{1}{T_{1A}} \right] = \frac{1}{T_{1m} + \tau_m} + \frac{1}{T_{1os}} \quad (11)$$

$$\frac{1}{T_{2r}} = \frac{1}{P_m} \left[\frac{1}{T_2} - \frac{1}{T_{2A}} \right] = \frac{1}{\tau_m} \frac{T_{2m}^{-2} + \tau_m^{-1} T_{2m}^{-1} + \Delta\omega_m^2}{(\tau_m^{-1} + T_{2m}^{-1})^2 + \Delta\omega_m^2} + \frac{1}{T_{2os}} \quad (12)$$

$$\Delta\omega_r = \frac{1}{P_m}(\omega - \omega_A) = \frac{\Delta\omega_m}{(1 + \tau_m T_{2m}^{-1})^2 + \tau_m^2 \Delta\omega_m^2} + \Delta\omega_{os} \quad (13)$$

where $1/T_{1m}$, $1/T_{2m}$ are the relaxation rates in the bound water, $\Delta\omega_m$ is the chemical shift difference between the bound and bulk water (in the absence of a paramagnetic interaction with the bulk water), P_m is the mole fraction of bound water, and τ_m is the residence time of water molecules in the inner coordination sphere. The total outer-sphere contributions to the reduced relaxation rates and chemical shift are represented by $1/T_{1os}$, $1/T_{2os}$ and $\Delta\omega_{os}$. The number of coordinated water molecules affects directly the value of P_m , and therefore to calculate the reduced relaxation rates and chemical shifts, $1/T_{1r}$, $1/T_{2r}$ and ω_r , the number of coordinated water molecules in the range of temperatures studied must be known. Although in diluted solutions ($\sim 10^{-3}$ M) the only species present in solution is the nona-coordinated one, this is not the case in the range of concentrations required for the ^{17}O NMR measurements. From the data reported in Table 4 we estimate $q = 2.8$ in a 0.037 M solution at 298 K. Furthermore, we assume that q is not changing with the temperature at a given concentration. This assumption is supported by the thermodynamic parameters reported in Table 4 at a concentration of 9×10^{-3} M. Under these conditions, the concentration of octa-coordinated species varies from 0.01% at 278 K to $\sim 10\%$ at 358 K, which corresponds to q values ranging from 3.0 to 2.9. Therefore, the assumption of constancy of q with the temperature produces an error of only about 3%. The temperature dependence of the reduced relaxation rates and chemical shifts for $[\text{Gd}(\text{EDTA-PA}_2)]^+$ is shown in Fig. 6.

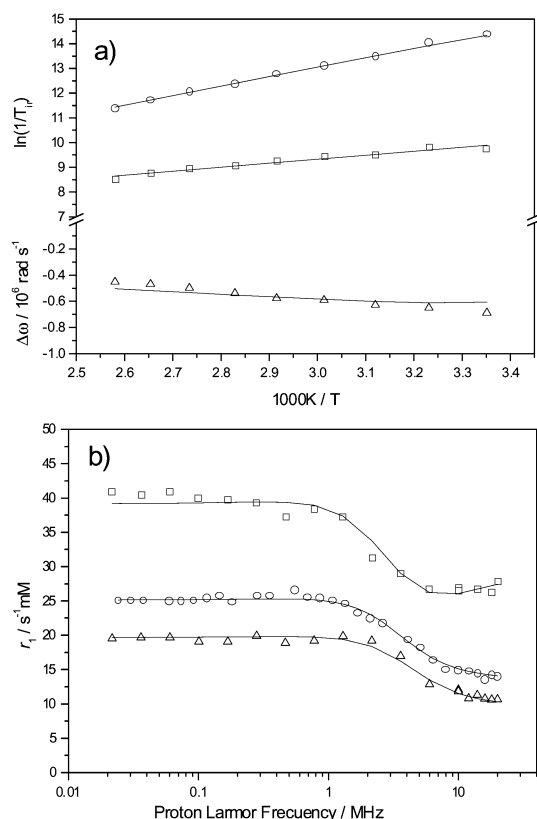


Fig. 6 Temperature dependence of (a) the reduced ^{17}O transverse (○) and longitudinal (□) relaxation rates of $[\text{Gd}(\text{EDTA-PA}_2)]^+$, expressed as $\ln(1/T_{1,2r})$, and the reduced chemical shifts, $\Delta\omega_r$ (Δ), and (b) NMRD profiles of $[\text{Gd}(\text{EDTA-PA}_2)]^+$ at 37 (Δ), 25 (○) and 5 °C (□).

It has been shown that the outer-sphere contributions in eqns. (11) and (12) can be neglected.^{39,40} Although the full eqns. (12) and (13) were used in the fit of the experimental data, it is

useful to consider the simplified eqns. (14) and (15), where the contribution of $\Delta\omega_m$ in eqn. (12) has been neglected.

$$\frac{1}{T_{1r}} = \frac{1}{T_{1m} + \tau_m} \quad (14)$$

$$\frac{1}{T_{2r}} = \frac{1}{T_{2m} + \tau_m} \quad (15)$$

Since τ_m decreases, while T_{1m} and T_{2m} generally increase with increasing temperature, the sign of the temperature dependence of $1/T_{1r}$ and $1/T_{2r}$ will depend on which term dominates in the denominator of eqns. (14) and (15). When a changeover exists from the “fast exchange” limit at high temperature, where T_{2m} is the principal term in the denominator of eqn. (15), to the slow exchange limit at low temperatures, where τ_m is the principal term, a maximum is observed in the temperature dependence of both $1/T_{1r}$ and $1/T_{2r}$. However, in the case of $[\text{Gd}(\text{EDTA-PA}_2)]^+$ $1/T_{1r}$ and $1/T_{2r}$ decrease with increasing the temperature, which indicates that T_{1m} and T_{2m} dominate the denominator of eqns. (14) and (15). This is characteristic of species in the fast exchange regime in the whole range of temperatures studied. Under these conditions, the inner-sphere contribution to $\Delta\omega_r$ is given by the chemical shift of the bound water molecules, which is determined by the hyperfine interaction between the Gd^{3+} electron spin and the ^{17}O nucleus *via* eqn. (16),⁴¹

$$\Delta\omega_m = \frac{g_L \mu_B S(S+1) B A}{3k_B T} \frac{1}{h} \quad (16)$$

where g_L is the isotropic Landé g -factor ($g_L = 2.0$ for Gd^{3+}), S is the electron spin ($S = 7/2$ for Gd^{3+}), A/h is the hyperfine or scalar coupling constant, and B is the magnetic field. We assume that the outer-sphere contribution to $\Delta\omega_r$ has temperature dependence similar to $\Delta\omega_m$ and is given by:

$$\Delta\omega_{os} = C_{os} \Delta\omega_m \quad (17)$$

where C_{os} is an empirical constant.⁴

The ^{17}O longitudinal relaxation rates in Gd^{3+} solutions are dominated by the dipole-dipole and quadrupolar mechanisms³⁹ and, to a good approximation,⁴⁰ may be expressed by:

$$\frac{1}{T_{1m}} = \left[\frac{1}{15} \left(\frac{\mu_0}{4\pi} \right)^2 \frac{\hbar^2 \gamma_I^2 \gamma_S^2}{r_{\text{GdO}}^6} S(S+1) \right] \times \left[6\tau_{\text{d1}} + 14 \frac{\tau_{\text{d2}}}{1 + \omega_S^2 \tau_{\text{d2}}} \right] + \frac{3\pi^2}{10} \frac{2I+3}{I^2(2I-1)} \chi^2 (1 + \eta^2/3) \tau_R \quad (18)$$

where $\gamma_S = g_L \mu_B / \hbar$ is the electron gyromagnetic ratio ($\gamma_S = 1.76 \times 10^{11} \text{ rad s}^{-1} \text{ T}^{-1}$ for $g_L = 2.0$), γ_I is the nuclear gyromagnetic ratio ($\gamma_I = -3.626 \times 10^7 \text{ rad s}^{-1} \text{ T}^{-1}$ for ^{17}O), r_{GdO} is the distance between the electron charge and the ^{17}O nucleus (the metal-oxygen distance in the point dipole approximation), τ_R is the rotational correlation time for the Gd^{3+} -O vector, $\tau_{\text{d1}}^{-1} = \tau_m^{-1} + T_{1e}^{-1} + \tau_R^{-1}$, I is the nuclear spin ($I = 5/2$ for ^{17}O), χ is the quadrupolar coupling constant, and η is an asymmetry parameter.

We assume that the rotational correlation time, τ_R , has a simple exponential temperature dependence as in eqn. (19), where τ_R^{298} is the correlation time at 298.15 K and E_R is the activation energy.

$$\tau_R = \tau_R^{298} \exp \left[\frac{E_R}{R} \left(\frac{1}{T} - \frac{1}{298.15} \right) \right] \quad (19)$$

The ^{17}O transverse relaxation rates in Gd^{3+} bound water molecules are dominated by the scalar relaxation mechanism⁴² and obey to a very good approximation (eqn. (20)) where $\tau_{\text{is}}^{-1} = \tau_{\text{m}}^{-1} + T_{\text{ie}}^{-1}$. It should be noted that the scalar mechanism is unimportant in the longitudinal relaxation and in proton relaxations.

$$\frac{1}{T_{2\text{m}}} = \frac{S(S+1)}{3} \left(\frac{A}{\hbar} \right)^2 \left(\tau_{\text{is}} + \frac{\tau_{2\text{s}}}{1 + \omega_{\text{s}}^2 \tau_{2\text{s}}^2} \right) \quad (20)$$

The residence time (or exchange rate, k_{ex}) of water molecules in the inner-sphere is assumed to obey the Eyring equation as written in eqn. (21), where ΔH^\ddagger is the enthalpy of activation for the exchange process and k_{ex}^{298} is the exchange rate at 298.15 K.

$$\frac{1}{\tau_{\text{m}}} = k_{\text{ex}} = \frac{k_{\text{ex}}^{298} T}{298.15} \exp \left[\frac{\Delta H^\ddagger}{R} \left(\frac{1}{298.15} - \frac{1}{T} \right) \right] \quad (21)$$

The electronic rates ($1/T_{\text{ie}}$) were approximated using eqns. (22) and (23):^{41,43}

$$\left(\frac{1}{T_{\text{ie}}} \right) = \frac{1}{2} \Delta^2 \tau_{\text{v}} [4S(S+1) - 3] \times \left(\frac{1}{1 + \omega_{\text{s}}^2 \tau_{\text{v}}^2} + \frac{4}{1 + 4\omega_{\text{s}}^2 \tau_{\text{v}}^2} \right) \quad (22)$$

$$\left(\frac{1}{T_{2\text{e}}} \right) = \Delta^2 \tau_{\text{v}} \left(\frac{5.26}{1 + 0.372\omega_{\text{s}}^2 \tau_{\text{v}}^2} + \frac{7.18}{1 + 1.24\omega_{\text{s}}^2 \tau_{\text{v}}^2} \right) \quad (23)$$

where ω_{s} is the Larmor frequency, Δ^2 is the trace of the square of the ZFS tensor, and τ_{v} is the correlation time for the modulation of ZFS. The modulation of the ZFS may be due to the modulation of transient distortions,⁴⁴ and we assume that the correlation time has Arrhenius behaviour (eqn. (24)).

$$\tau_{\text{v}} = \tau_{\text{v}}^{298} \exp \left[\frac{E_{\text{v}}}{R} \left(\frac{1}{T} - \frac{1}{298.15} \right) \right] \quad (24)$$

Variable-temperature NMRD measurements. The $[\text{Gd}(\text{EDTA-PA}_2)]^+$ chelate was investigated by water ^1H longitudinal relaxation time measurements at 5, 25 and 37 °C and magnetic field strengths varying between 2.16×10^{-3} and 0.47 T (NMRD), and the curves obtained are included in Fig. 6. Longitudinal proton relaxation enhancements in NMRD studies are commonly expressed in relaxivities (r_1 , in $\text{s}^{-1} \text{mM}^{-1}$). The relation between r_1 and the inner- and outer-sphere contributions is given by eqn. (11) with $P_{\text{m}} = (cq)/55.5$, where c is the Gd^{3+} concentration in mol L^{-1} and q is the number of inner-sphere water molecules ($q = 3$ for $[\text{Gd}(\text{EDTA-PA}_2)]^+$ at a concentration of 10^{-3} M). The longitudinal relaxation rate of the inner-sphere water molecules is dominated by the dipolar interaction and is given by the Solomon-Bloembergen equation (eqn. (25)):⁴⁵⁻⁴⁷

$$\frac{1}{T_{1\text{m}}} = \frac{2}{15} \left(\frac{\mu_0}{4\pi} \right)^2 \frac{\hbar^2 \gamma_{\text{s}}^2 \gamma_{\text{i}}^2}{r_{\text{GdH}}^2} S(S+1) \left(\frac{3\tau_{\text{d1}}}{1 + \omega_{\text{i}}^2 \tau_{\text{d1}}^2} + \frac{7\tau_{\text{d2}}}{1 + \omega_{\text{s}}^2 \tau_{\text{d2}}^2} \right) \quad (25)$$

$$r_{\text{ios}} = \left(\frac{32\pi}{405} \right) \left(\frac{\mu_0}{4\pi} \right)^2 \gamma_{\text{i}}^2 \gamma_{\text{s}}^2 \hbar^2 S(S+1) \frac{N_{\text{A}}}{a_{\text{GdH}} D_{\text{GdH}}} [3J_{\text{Os}}(\omega_{\text{i}}, T_{\text{ie}}) + 7J_{\text{Os}}(\omega_{\text{s}}, T_{2\text{e}})] \quad (26)$$

$$J_{\text{Os}}(\omega, T_{\text{je}}) = \text{Re} \left\{ \left\{ 1 + \frac{1}{4} [i\omega\tau_{\text{GdH}} + (\tau_{\text{GdH}}/T_{\text{je}})]^{1/2} \right\} \left\{ 1 + [i\omega\tau_{\text{GdH}} + (\tau_{\text{GdH}}/T_{\text{je}})]^{1/2} + \frac{4}{9} [i\omega\tau_{\text{GdH}} + (\tau_{\text{GdH}}/T_{\text{je}})] + \frac{1}{9} [i\omega\tau_{\text{GdH}} + (\tau_{\text{GdH}}/T_{\text{je}})]^{3/2} \right\} \right\} \quad (27)$$

where r_{GdH} is the effective distance between the gadolinium electronic spin and the water protons and $\tau_{\text{di}}^{-1} = \tau_{\text{M}}^{-1} + \tau_{\text{R}}^{-1} + T_{\text{ie}}^{-1}$ ($i = 1, 2$). The rotational correlation time (τ_{R}) now refers to the rotation of the Gd^{3+} -water proton vector.

The outer-sphere contribution to the relaxivity, arising from diffusing water molecules external to the chelate complex for a 1 mM solution, can be expressed by eqns. (26) and (27),⁴⁸ where $j = 1, 2$ and N_{A} is the Avogadro's number, a_{GdH} is the distance of the closest approach of a second-sphere water molecule to Gd^{3+} , and the correlation time τ_{GdH} corresponds with $a_{\text{GdH}}^2/D_{\text{GdH}}$. The diffusion coefficient D_{GdH} is assumed to obey an exponential temperature dependence (eqn. (28)),

$$D_{\text{GdH}} = D_{\text{GdH}}^{298} \exp \left[\frac{E_{D_{\text{GdH}}}}{R} \left(\frac{1}{298.15} - \frac{1}{T} \right) \right] \quad (28)$$

where D_{GdH}^{298} is the diffusion coefficient at 298.15 K and $E_{D_{\text{GdH}}}$ is the activation energy.

The temperature dependence of the NMRD profile usually gives a good indication of which parameter limits the proton relaxivity. If the high field value (>10 MHz) increases with increasing temperature, relaxivity is limited by slow water exchange, whereas in the opposite case fast rotation is the limiting factor. For $[\text{Gd}(\text{EDTA-PA}_2)]^+$, the relaxivity increases with decreasing the temperature which shows that the relaxivity is dominated by the fast rotation, as is usually observed for small Gd^{3+} chelates.^{3,49}

Simultaneous fitting of NMRD and ^{17}O NMR data. A simultaneous fitting of the NMRD and ^{17}O NMR data of $[\text{Gd}(\text{EDTA-PA}_2)]^+$ was performed according to eqns. (11)–(28). The following strategy was adopted: a_{GdH} , the distance of closest approach for the outer-sphere contribution was set at 0.35 nm and, following previous NMRD studies, the distance between the protons of the coordinated water molecules and the Gd^{3+} ion, r_{GdH} was fixed at 0.31 nm.^{49,50} The r_{GdO} distance was also fixed at 0.25 nm. The number of water molecules in the first coordination sphere of Gd^{3+} , q , was taken as 3.0 for the NMRD equations. However, an effective $q = 2.8$ was used to determine the ^{17}O reduced relaxation rates and chemical shifts (see above). One might argue that a simultaneous fitting of the NMRD and ^{17}O NMR data is not the best approach in the present case, since some of the parameters (q and τ_{R}) have been shown to be concentration dependent (*vide supra*). However, independent fits of the ^{17}O NMR data have been shown to be quite insensitive to several fitting parameters due to the nearly linear dependence of the reduced relaxation rates and chemical shifts with the temperature. The validity of a simultaneous treatment of the NMRD and ^{17}O NMR data in this case is therefore based on the assumption that the residence time of water molecules in the inner coordination sphere of Gd^{3+} , τ_{m} , does not change significantly in the concentration range 1–37 mM. Because of the concentration dependence of the rotational correlation time, τ_{R} , observed from deuterium longitudinal relaxation rate measurements, we used two different rotational correlation times for the Gd–H (τ_{RH}) and Gd–O (τ_{RO}) vectors during the fitting procedure. Furthermore, it has been demonstrated,

Table 6 Parameters obtained from the simultaneous analysis of ^{17}O NMR and NMRD for the $[\text{Gd}(\text{EDTA-PA}_2)]^+$ complex

Parameter	Gd(EDTA-PA ₂)	Gd(DTPA-BMA) ^a
$k_{\text{ex}}/10^6 \text{ s}^{-1}$	44 ± 4	0.45 ± 0.01
$\Delta H^\ddagger/\text{kJ mol}^{-1}$	29 ± 1	47.6 ± 1.1
$A/\hbar/10^6 \text{ rad s}^{-1}$	-3.93 ± 0.05	-3.8 ± 0.2
$\tau_{\text{RH}}/298/\text{ps}$	113 ± 5	66 ± 11
$E_{\text{RH}}/\text{kJ mol}^{-1}$	18 ± 2	21.9 ± 0.5
$\tau_{\text{RO}}/298/\text{ps}$	117 ± 8	^c
$E_{\text{RO}}/\text{kJ mol}^{-1}$	13 ± 1	^c
$\tau_{\text{v}}/298/\text{ps}$	36 ± 4	25 ± 1
$E_{\text{v}}/\text{kJ mol}^{-1}$	1 ^b	3.9 ± 1.4
$A^2/10^{20} \text{ s}^{-2}$	0.16 ± 0.02	0.41 ± 0.02
$D_{\text{GdH}}/10^{-10} \text{ m}^2 \text{ s}^{-1}$	18 ± 3	23 ± 2
$E_{\text{DGdH}}/\text{kJ mol}^{-1}$	52 ± 4	12.9 ± 2.1
$\chi(1 + \eta^2)^{1/2}/\text{MHz}$	7.58 ^b	7.58 ^b

^a The data listed for [Gd(DTPA-BMA)] have been reported previously in ref. 4 and are provided here for comparison. ^b Parameters fixed during the fitting procedure. ^c Only one rotational correlation time for both Gd-H and Gd-O vectors was used.

both experimentally and by molecular dynamics simulations, that $\tau_{\text{RH}}/\tau_{\text{RO}} = 0.65\text{--}0.75$ in several Gd^{3+} complexes of poly(aminocarboxylates).^{51,52} The results of the fits are presented in Table 6 and are also shown in Fig. 6.

It has been observed that the water-exchange rate decreases dramatically from $[\text{Gd}(\text{H}_2\text{O})_8]^{3+}$ to the chelate complexes with one inner-sphere water molecule.⁴ In the case of the $[\text{Gd}(\text{EDTA-PA}_2)]^+$ complex the water-exchange rate is about 18 times smaller than for $[\text{Gd}(\text{H}_2\text{O})_8]^{3+}$, but about 100 times faster than for [Gd(DTPA-BMA)], which contains a single inner-sphere water molecule (see Table 6). The water exchange rate determined for $[\text{Gd}(\text{EDTA-PA}_2)]^+$ is also *ca.* 4.5 times faster than that reported for $[\text{Er}(\text{EDTA})]^-$ ($9.8 \times 10^6 \text{ s}^{-1}$).⁷ These data contrast with previous observations for related systems which showed that an increase of the net charge from -1 to +1 is accompanied by a decrease in the water exchange rate of one order of magnitude.⁵³ Apparently, other factors than the net charge of the complex have a more important impact on the water exchange rates.⁵⁴

From the data reported in Fig. 2, we estimate rotational correlation times of 106 and 120 ps at concentrations of 1 mM and 37 mM respectively, in excellent agreement with the values obtained from the simultaneous fitting ($\tau_{\text{RH}}^{298} = 113 \text{ ps}$ and $\tau_{\text{RO}}^{298} = 117 \text{ ps}$).

The good quality of the fittings obtained from the simultaneous treatment of the NMRD and ^{17}O NMR data and the reasonable parameters obtained gives us confidence that the water exchange rate does not vary much with the concentration in the range 1–37 mM. Moreover, the correctness of the assumption of a hydration number of $q = 2.8$ for the ^{17}O NMR data is confirmed by the value obtained for the scalar coupling constant (A/\hbar), which is similar to values reported for other Gd^{3+} polyaminocarboxylate complexes.¹

Conclusions

This study shows that the hydration number, q , of $[\text{Ln}(\text{EDTA-PA}_2)]^+$ complexes in aqueous solutions is dependent the concentration of the complex. The substitution of two carboxylates of EDTA with amide functionalities strongly influences some properties of the Ln^{3+} complexes including their stability. ^{13}C NMR studies demonstrate that the complexes exist in solution as a mixture of *cis* and *trans* isomers. The presence of intermolecular interactions, that are especially important in concentrated solutions, have been demonstrated by different NMR techniques. These interactions are responsible for the concentration dependence of some parameters that affect the proton relaxivity such as the rotational correlation time,

τ_{R} , and the number of inner-sphere water molecules, q . We believe that these intermolecular interactions may also operate in other cationic Gd^{3+} chelates and, therefore, caution is needed when different techniques that require a different concentration range are used to study the parameters governing the ^1H relaxivity. At 37 °C, the fast rotation is the limiting factor for the inner-sphere relaxivity of the $[\text{Gd}(\text{EDTA-PA}_2)]^+$ complex.

Experimental

^1H (300 MHz), ^{13}C (75.5 MHz), ^{17}O (40.7 MHz) and ^2H (46.1 MHz) NMR spectra were recorded on a Varian INOVA-300 spectrometer with 5 mm or 10 mm tubes (^2H). Chemical shifts are reported as δ values. For measurements in D_2O , *tert*-butyl alcohol was used as an internal standard with the methyl signal calibrated at $\delta = 1.2 \text{ ppm}$ (^1H) or 31.2 (^{13}C). D_2O (100%) was used as an external chemical shift reference for ^{17}O resonances. Samples of the Ln^{3+} complexes for the ^{13}C and ^{17}O NMR measurements were prepared by mixing of equimolar amounts of EDTA-PA₂ and hydrated LnCl_3 (Aldrich Chemical Co.) in D_2O , followed by the adjustment of the pD to *ca.* 6 with a solution of NaOD in D_2O . ^{89}Y (19.6 MHz) NMR spectra were recorded on a Varian VXR-400 S spectrometer using 5 mm sample tubes. A 2 M YCl_3 solution was used as external reference. The pH of the solutions was measured at room temperature with a calibrated microcombination probe purchased from Aldrich Chemical Co. The pH values given are direct meter readings without correction for D-isotope effects. The solvent (water) for deuterium longitudinal relaxation rates was deuterium depleted. Longitudinal relaxation rates ($1/T_1$) were determined by the inversion-recovery method,⁵⁵ and the transverse relaxation rates ($1/T_2$) were obtained by the Carr-Purcell-Meiboom-Gill spin-echo technique.⁵⁶

The experimental details for high-resolution laser excited luminescence measurements were previously described.⁵⁷ Lifetimes are averages of at least 3–5 independent determinations. The $1/T_1$ nuclear magnetic relaxation dispersion (NMRD) profiles of the solvent protons at 5, 25 and 37 °C and 1 mM concentration were obtained on a Spinmaster FFC Fast Field Cycling NMR relaxometer (Stelar), covering a continuum of magnetic fields from 7×10^{-4} to 0.47 T (corresponding to a proton Larmor frequency range of 0.03–20 MHz). UV-Visible spectrophotometric measurements were made on a Perkin-Elmer Lambda 19 double beam spectrophotometer and the spectra were recorded in digital form. A thermostatable cylindrical cell with a long optical path (10 cm) was used, in order to maximise the observed absorption.

Potentiometry measurements

The ligand protonation constants and the stability constant of the Gd^{3+} complex were determined by pH-potentiometry at a constant ionic strength (0.1 M $(\text{CH}_3)_4\text{NCl}$). The titrations were carried out in a thermostated vessel ($25 \pm 0.2 \text{ }^\circ\text{C}$) using $(\text{CH}_3)_4\text{NOH}$ as titrant solution dosed with a Metrohm Dosimat 665 automate burette. A combined glass electrode (C14/02-SC, reference electrode Ag/AgCl in 3 M KCl, Moeller Scientific Glass Instruments, Switzerland) connected to a Metrohm 692 pH/ion-meter was used to measure pH. The titrated solution (3 mL) was stirred with a magnetic stirrer and bubbled with a constant N_2 flow. Protonation and stability constants were determined at 0.002 M ligand concentration from 3–4 parallel titrations. Since the Gd^{3+} complex is almost completely formed at low pH, the stability constant was obtained by ligand competition between EDTA-PA₂ and EDTA, at a metal : EDTA : EDTA-PA₂ ratio of 1 : 1 : 1. The hydrogen ion concen-

tration was calculated from the measured pH values using the correction method suggested by Irving *et al.*⁵⁸ All protonation and stability constants were computed with the program PSEQUAD.⁵⁹

Synthesis of EDTA-PA₂

Ethylenediaminetetraacetic acid (20.0 g, 68 mmol) was combined with acetic anhydride (32 g, 312 mmol) and dry pyridine (34 mL) in a round bottom flask equipped with stirrer bar and condenser. The mixture was heated at 65 °C for 72 h and then cooled to room temperature. The suspension obtained was filtered and the solids were washed with diethyl ether. After drying *in vacuo* over KOH, a 16 g amount of EDTA-bis(anhydride) (62.4 mmol) was obtained, which was dissolved in 125 mL of DMF. To the stirred solution, two equivalents of triethylamine was added. The propylamine (7.4 g, 125 mmol) was added dropwise and the stirring was continued for 24 h at ambient temperature. Then the mixture was concentrated by rotary evaporation leaving a brown solid residue. The crude product was treated with isopropyl alcohol, which dissolved the coloured impurities, leaving a white solid. The solid was collected, washed with isopropyl alcohol and dried *in vacuo* yielding 15.3 g of EDTA-PA₂ (66%); mp 153–154 °C; [Found: C, 51.0; H, 7.9; N, 14.8. Calc. for C₁₆H₃₀N₄O₆: C, 51.3; H, 8.1; N, 15.0%]. δ_{H} (D₂O, pH 7): 0.92 (6 H, t), 1.57 (4 H, m.), 3.25 (8 H, m), 3.55(4 H, s) and 3.78(4 H, s); δ_{C} (D₂O, pH 7): 12.2, 23.4, 42.8, 53.5, 58.5, 58.9, 171.2, 176.3.

Synthesis of EDTA-PA₂-d₄

Deuteration of EDTA-PA₂ at the α -position respect to carbonyl groups of the acetate pendant arms was carried out by a similar procedure to that described in the literature.⁶⁰ 0.5 mmol of ligand was dissolved in 20 mL of D₂O, the pD was adjusted to 10.6 by addition of solid K₂CO₃, and the mixture was stirred and heated to reflux for 24 h. The pH was then adjusted to 2 with a 25% HCl solution, the solution of the ligand concentrated to 10 mL and 10 mL of EtOH were added. The precipitated KCl was filtered off, and the solution concentrated to dryness. The resultant solid residue was treated with 10 mL of MeOH, the solution filtered and the filtrate concentrated to dryness and dried under vacuum at room temperature overnight. The deuteration was confirmed by ¹H NMR spectroscopy (>95%).

Acknowledgements

This research was performed within the framework of the EU COST Action "Lanthanide Chemistry for diagnosis and therapy" (D18).

References

- 1 A. E. Merbach and É. Tóth (Editors), *The Chemistry of Contrast Agents in Medical Magnetic Resonance Imaging*, John Wiley & Sons, Chichester, 2001.
- 2 J. A. Peters, J. Huskens and D. J. Raber, *Prog. Magn. Reson. Spectrosc.*, 1996, **28**, 283.
- 3 P. Caravan, J. J. Ellison, T. J. McMurphy and R. B. Lauffer, *Chem. Rev.*, 1999, **99**, 2293.
- 4 D. H. Powell, O. M. Ni Dhubhghaill, D. Pubanz, L. Helm, Y. S. Lebedev, W. Schlaepfer and A. E. Merbach, *J. Am. Chem. Soc.*, 1996, **118**, 9333.
- 5 C. M. Dobson, R. J. P. Williams and A. V. Xavier, *J. Chem. Soc., Dalton Trans.*, 1974, 1762.
- 6 A. D. Sherry, P. P. Yang and L. O. Morgan, *J. Am. Chem. Soc.*, 1980, **102**, 5755.
- 7 N. Graeppe, D. H. Powell, G. Laurency, L. Zékány and A. E. Merbach, *Inorg. Chim. Acta*, 1995, **235**, 311.

- 8 P. Caravan, P. Mehrkhodavandi and C. Orvig, *Inorg. Chem.*, 1997, **36**, 1316.
- 9 Y.-M. Wang, Y.-J. Wang and Y.-L. Wu, *Polyhedron*, 1998, **18**, 109.
- 10 IUPAC Stability constants. Academic Software, K. J. Powell, 1999.
- 11 B. M. Alsaadi, F. J. C. Rossotti and R. J. P. Williams, *J. Chem. Soc., Dalton Trans.*, 1980, 2151.
- 12 I. Bertini, F. Capozzi, C. Luchinat, G. Nicastro and Z. Xia, *J. Phys. Chem.*, 1993, **97**, 6351.
- 13 J. A. Peters, *Inorg. Chem.*, 1988, **27**, 4686.
- 14 C. F. G. C. Geraldes, A. M. Urbano, M. A. Hoefnagel and J. A. Peters, *Inorg. Chem.*, 1993, **32**, 2426.
- 15 H. Lammers, F. Maton, D. Pubanz, M. W. van Laren, H. van Bekkum, A. E. Merbach, R. N. Muller and J. A. Peters, *Inorg. Chem.*, 1997, **36**, 2527.
- 16 J. Reuben and D. Fiat, *J. Chem. Phys.*, 1969, **51**, 4918.
- 17 M. Gueron, *J. Magn. Reson.*, 1975, **19**, 58.
- 18 A. J. Vega and D. Fiat, *Mol. Phys.*, 1976, **31**, 374.
- 19 E. J. Corey and J. C. Bailar, Jr., *J. Am. Chem. Soc.*, 1959, **81**, 2620.
- 20 L. Vander Elst, S. Laurent and R. N. Muller, *Invest. Radiol.*, 1998, **33**, 828.
- 21 H. H. Mantsch, H. Saito and I. C. P. Smith, *Prog. Nucl. Magn. Reson. Spectrosc.*, 1977, **11**, 211.
- 22 W. Derbyshire, T. C. Gorvin and D. Warner, *Mol. Phys.*, 1969, **17**, 401.
- 23 T. K. Hitchens and R. G. Bryant, *J. Phys. Chem.*, 1995, **99**, 5612.
- 24 W. D. Horrocks, Jr. and D. R. Sudnick, *J. Am. Chem. Soc.*, 1979, **101**, 334.
- 25 A. Beeby, I. M. Clarkson, R. S. Dickins, S. Faulkner, D. Parker, L. Royle, A. S. de Sousa, J. A. G. Williams and M. Woods, *J. Chem. Soc., Perkin Trans. 2*, 1999, 493.
- 26 R. M. Supkowski and W. D. Horrocks, Jr., *Inorg. Chim. Acta.*, 2002, **340**, 44.
- 27 S. T. Frey and W. DeW. Horrocks, Jr., *Inorg. Chim. Acta*, 1995, **229**, 383.
- 28 C. A. M. Vijverberg, J. A. Peters, A. P. G. Kieboom and H. van Bekkum, *Trav. Chim. Pays-Bas*, 1980, **99**, 403.
- 29 J. A. Peters, M. S. Nieuwenhuizen and D. J. Raber, *J. Magn. Reson.*, 1985, **65**, 417.
- 30 M. S. Nieuwenhuizen, J. A. Peters, A. Sinnema, A. P. G. Kieboom and H. van Bekkum, *J. Am. Chem. Soc.*, 1985, **107**, 12.
- 31 M. C. Alpoim, A. M. Urbano, C. F. G. C. Geraldes and J. A. Peters, *J. Chem. Soc., Dalton Trans.*, 1992, 463.
- 32 R. M. Golding and M. P. Halton, *Aust. J. Chem.*, 1972, **25**, 2577.
- 33 B. Bleaney, *J. Magn. Reson.*, 1972, **25**, 2577.
- 34 B. Bleaney, C. M. Dobson, B. A. Levine, R. B. Martin, R. J. P. Williams and A. V. Xavier, *J. Chem. Soc., Chem. Commun.*, 1972, 791.
- 35 J. R. Zimmerman and W. E. Brittin, *J. Phys. Chem.*, 1957, **61**, 1328.
- 36 T. J. Swift and R. E. Connick, *J. Chem. Phys.*, 1962, **37**, 307.
- 37 J. S. Leigh, Jr., *J. Magn. Reson.*, 1971, **4**, 308.
- 38 A. C. McLaughlin and J. S. Leigh, Jr., *J. Magn. Reson.*, 1973, **9**, 296.
- 39 K. Micskei, L. Helm, E. Brücher and A. E. Merbach, *Inorg. Chem.*, 1993, **32**, 3844.
- 40 K. Micskei, D. H. Powell, L. Helm, E. Brücher and A. E. Merbach, *Magn. Reson. Chem.*, 1993, **31**, 1011.
- 41 A. D. McLachlan, *Proc. R. Soc. London, A*, 1964, **280**, 271.
- 42 R. V. Southwood-Jones, W. L. Earl, K. E. Newman and A. E. Merbach, *J. Chem. Phys.*, 1980, **73**, 5909.
- 43 D. H. Powell, A. E. Merbach, G. González, E. Brücher, K. Micskei, M. F. Ottaviani, K. Köhler, A. Von Zelewsky, O. Ya. Grinberg and Ya. S. Lebedev, *Helv. Chim. Acta*, 1993, **76**, 2129.
- 44 L. Friedman, in *Protons and Ions Involved in Fast Dynamics Phenomena*, ed. P. Laszlo, Elsevier, Amsterdam, 1978, pp. 27–42.
- 45 N. Bloembergen, *J. Chem. Phys.*, 1957, **27**, 595.
- 46 I. Solomon, *Phys. Rev.*, 1955, **99**, 559.
- 47 N. Bloembergen and L. O. Morgan, *J. Chem. Phys.*, 1961, **34**, 842.
- 48 J. H. Freed, *J. Chem. Phys.*, 1978, **68**, 4030.
- 49 S. H. Koenig and R. D. Brown., *Magn. Reson. Med.*, 1984, **1**, 478.
- 50 C. F. G. C. Geraldes, A. M. Urbano, M. C. Alpoim, A. D. Sherry, K.-T. Kuan, R. Rajagopalan, F. Maton and R. N. Muller, *Magn. Reson. Imaging*, 1995, **2**, 13.
- 51 F. A. Dunand, A. Borel and A. E. Merbach, *J. Am. Chem. Soc.*, 2002, **124**, 710.
- 52 F. Yerly, K. I. Hardcastle, L. Helm, S. Aime, M. Botta and A. E. Merbach, *Chem. Eur. J.*, 2002, **8**, 1031.

-
- 53 S. Aime, A. Barge, M. Botta, L. Frullano, U. Merlo and K. I. Hardcastle, *J. Chem. Soc., Dalton Trans.*, 2000, 3435.
- 54 F. Botteman, G. M. Nicolle, L. Vander Elst, S. Laurent, A. E. Merbach and R. N. Muller, *Eur. J. Inorg. Chem.*, 2002, 2686.
- 55 R. V. Vold, J. S. Waugh, M. P. Klein and D. E. Phelps, *J. Chem. Phys.*, 1968, **48**, 3831.
- 56 S. Meiboom and D. Gill, *Rev. Sci. Instrum.*, 1958, **29**, 688.
- 57 R. Rodríguez-Cortiñas, F. Avecilla, C. Platas-Iglesias, D. Imbert, J.-C. G. Bünzli, A. de Blas and T. Rodríguez-Blas, *Inorg. Chem.*, 2002, **41**, 5336.
- 58 H. Irving, M. G. Miles and L. Pettit, *Anal. Chim. Acta*, 1967, **38**, 475.
- 59 L. Zékány and I. Nagypál, in *Computational methods for determination of formation constants*, ed. D. J. Leggett, Plenum Press, N.Y., 1985, p. 291.
- 60 W. D. Wheeler and J. J. Legg, *Inorg. Chem.*, 1985, **24**, 129.